GNSS Receiver Bias Model for Near Real Time TEC Monitoring at Low Latitude, Thailand

Prasert Kenpankho[*,1], Samatchaya Maichuen[1], Prarinya Phothila[1], Jianfeng Zhang[1], Thanapon Keokhumcheng[2], Sontaya Ruttanaburee[3], Patinya Pornsopin[3]

[(1)] Department of Engineering Education, School of Industrial Education and Technology, King Mongkut's Institute of Technology Ladkrabang, Bangkok 10520, Thailand

[(2)] Department of Electronics, Nongbualumphu Technical College, Institute of Vocational Education Northeastern Region 1. Nongbualumphu, 39000, Thailand

[(3)] Earthquake Observation Division, Thai Meteorological Department, Bangkok 10260, Thailand

Abstract

This research proposes and investigates GNSS receiver bias modeling for near real time total electron content (TEC) monitoring across 16 multi-frequency GNSS stations in low latitude, Thailand, from 2022-2024. By applying a refined methodology based on Kenpankho et al. (2021) and integrating IONOLAB-BIAS for single station bias estimation, the research corrects for satellite and receiver inter-frequency biases to enhance TEC accuracy. Results show a consistent upward trend in TEC values, reflecting increased latitudes, seasonal ionospheric activity, and geomagnetic storms. Comparative analysis with the IRI 2020 model using correlation coefficients and RMSE reveals spatial and temporal variation, with near equatorial latitude stations showing strong alignment than upper low latitude stations. The results highlight the importance of localized GNSS-based TEC models for improving satellite positioning accuracy in equatorial regions and highlight the limitations of global models under dynamic ionospheric conditions.

Keywords: GNSS receiver bias; TEC; IRI TEC; Low latitude

1. Introduction

In recent years, multi-frequency signals from the Global Navigation Satellite System (GNSS) have become a fundamental tool for estimating Total Electron Content (TEC) at both regional and global scales. TEC is derived from the time delay experienced by GNSS signals as they propagate through the ionosphere and are received by ground-based stations. The BeiDou satellite system, developed by China, and the GPS system, developed by the United States, are both part of GNSS. Thailand can receive signals from both satellite constellations for positioning and various practical applications. Although satellite receivers have been significantly improved for higher accuracy, several external factors still cause signal errors. These errors affect the transmission of satellite signals to Earth, resulting in deviations in positioning accuracy. One of the most critical sources of error is the ionosphere, a layer of the atmosphere located approximately 50 to 1,000 kilometers above the Earth's surface. This layer plays a vital

role in satellite communication and contains a high concentration of free electrons. The constant fluctuation of these electrons causes signal delays, which in turn lead to inaccuracies in the reception of BeiDou and GPS signals. Consequently, positioning results may deviate from the predicted values.

Numerous studies have explored the behavior of BeiDou and GPS signals in relation to ionospheric effects. For example, Ma and Maruyama (2003) investigated the origin of TEC and instrument bias using GEONET data in Japan, finding that GPS satellite and receiver biases were generally stable. Kenpankho et al. (2011) estimated TEC and receiver delay times using GEONET data in Japan. Zhang et al. (2015) developed a regional ionospheric delay model using BeiDou and GPS observations in China. Li et al. (2015) examined high-precision positioning using GPS, GLONASS, Galileo, and BeiDou systems. Absolute TEC can be determined by analyzing the differential delay between the two GNSS code frequencies. For applications requiring high-precision positioning and accurate TEC estimation, it is essential to correct for inter-frequency biases originating from both satellites and receivers (Otsuka et al., 2002; Warnant, 1997). These receiver-related biases are variously referred to in the literature as instrumental bias, differential bias, receiver offset, differential code bias (DCB), and inter-frequency bias (IFB). Further research includes Dandan et al. (2017), who proposed methods for correcting ionospheric delay effects, and Srivani et al. (2019), who applied deep learning techniques to predict ionospheric delays for GPS signals. Mallika et al. (2020) studied machine learning algorithms for predicting ionospheric delay times. Wang et al. (2021) evaluated the performance of the BeiDou Global Ionospheric Delay Correction Model (BDGIM) under different solar conditions. Cao et al. (2021) analyzed delay times between BeiDou-2 and BeiDou-3 satellites. Xiao et al. (2022) developed and assessed atmospheric delay models for GPS, Galileo, and BDS PPP-RTK applications at the regional level.

Based on a comprehensive review of related research, particularly those focused on TEC in the ionosphere, this study adopts the methodology proposed by Kenpankho et al. (2011) for comparing GPS signal delay times derived from TEC calculations. This approach is adapted to analyze the GNSS receiver biases of BeiDou and GPS signals affected by ionospheric conditions. To address these biases, several methods have been developed. Multi-station approaches typically involve modeling TEC using double-difference GPS observations, which help isolate and estimate differential biases (Makela et al., 2001; Sardon et al., 1994; Warnant, 1997). For single-station bias estimation, two primary methodologies are commonly cited. The first involves modeling TEC as a polynomial function of coordinates in the Earth-Sun reference frame, incorporating both satellite and receiver biases. These unknowns are solved using a least squares approach (Coco et al., 1991; Jakowski et al., 1996; Lanyi and Roth, 1988; Otsuka et al., 2002; Warnant, 1997). In the second method, TEC is computed from different satellites over a certain angle of elevation, and the computed TEC values are considered be close to each other. This proximity is found by calculating standard deviation of TEC obtained from all satellites. To obtain the optimum receiver bias value, trial receiver biases are used in TEC computation and the receiver bias that minimizes the standard deviation is chosen as the receiver bias value for that GPS station (Ma and Maruyama, 2003; Zhang et al., 2003).

This research aims to study GNSS receiver bias model for near real time TEC monitoring at low latitude, Thailand using GNSS signals collected from 16 multi-frequency GNSS receiving stations in Thailand. The collected data are used to calculate and compare delay times for both satellite systems, contributing to improved understanding and modeling of ionospheric effects on satellite-based positioning. The data are examined on the period of the year 2022-2024 and compared with the International Reference Ionosphere (IRI) model (Kenpankho et al., 2011; Kenpankho et al., 2021; Keokhumcheng and Kenpankho, 2025). This ensures that the proposed model analysis meets international standards.

2. Data and Methodology

This research introduces a GNSS receiver bias model designed to enable near real-time estimation of Total Electron Content (TEC) using data from GNSS receiver stations positioned along low-latitude lines crossing Thailand. The proposed model is evaluated against two established techniques: the polynomial fitting method and the standard deviation minimization approach. Its primary goal is to simplify and accelerate the estimation of receiver biases for GNSS satellites by using receiver bias data as the constants with 15 minutes interval. To support timely TEC monitoring, the model employs Lagrange interpolation for calculating derivatives and integrals of discrete receiver bias data. This approach enhances computational efficiency while maintaining accuracy in bias correction for both satellite systems.

2.1 16 GNSS stations in low latitude, Thailand

In this research, there are 16 GNSS receiver stations at low latitude, Thailand, as follows: BANG (Bangkok) (13.40 N, 100.36 E, Dip 4.17 N), MAIG (Chiangmai) (19.21 N, 99.12 E Dip 13.34 N), CRAI (Chiangrai) (19.57 N, 99.52 E, Dip 13.74 N), KANN (Kanchanaburi) (14.10 N, 99.31 E, Dip 7.69 N), KABG (Krabi) (8.06 N, 98.58 E, Dip 0.17 N), LAMG (Lampang) (18.03 N, 99.14 E, Dip 12.04 N), MAEH (Maehongson) (19.18 N, 97.58 E, Dip 13.30 N), MHSG (MaeSariang) (18.10 N, 97.55 E, Dip 12.11 N), NANN (Nan) (18.46 N, 100.458 E, Dip 12.53 N), PHAG (Phangna) (8.41 N, 98.15 E, Dip 0.22 N), PHEG (Phetchabun) (15.46 N, 101.01 E, Dip 9.22 N), PRAG (Prachuapkhirikhan) (11.56 N, 99.41 E, Dip 4.80 N), UTHG (Uthaithani) (15.21 N, 100.00 E, Dip 8.93 N), MMAI (MaeChaem, Chiangmai) (18.50 N, 98.36 E, Dip 12.56 N), KMITL Chumphon (King Mongkut's Institute of Technology Ladkrabang Chumphon Campus) (10.73 N, 99.37 E, Dip 3.82 N), and SIET KMITL (School of Industrial Education and Technology, King Mongkut's Institute of Technology Ladkrabang) (13.73 N, 100.78 E, Dip 7.28 N) shown as Table 1.

Table 1. 16 GNSS receiver stations with station code, location, and coordination.

Station code	Location	Geomagnetic Latitude (°N)	Latitude (°N)	Longitude (°E)
1. BANG	Bangkok	4.17	13.40	100.36
2. MAIG	Chiangmai	13.34	19.21	99.12
3. CRAI	Chiangrai	13.74	19.57	99.52
4. KANN	Kanchanaburi	7.69	14.10	99.31
5. KABG	Krabi	0.17	8.06	98.58
6. LAMG	Lampang	12.04	18.03	99.14
7. MAEH	Maehongson	13.30	19.18	97.58
8. MHSG	MaeSariang	12.11	18.10	97.55
9. NANN	Nan	12.53	18.46	100.458
10. PHAG	Phangnga	0.22	8.41	98.15
11. PHEG	Phetchabun	9.22	15.46	101.01
12. PRAG	Prachuapkhirikhan	4.80	11.56	99.41
13. UTHG	Uthaithani	8.93	15.21	100.00
14. MMAI	MaeChaem, Chiangmai	12.56	18.50	98.36
15. KMITL Chumphon	King Mongkut's Institute of Technology Ladkrabang Chumphon Campus	3.82	10.73	99.37
16. SIET KMITL	School of Industrial Education and Technology, King Mongkut's Institute of Technology Ladkrabang	7.28	13.73	100.78

The GNSS receiver stations with station code are on the map as color station codes and black star signs shown in Fig. 1. The data used for the model spans the period from 2022 to 2024, based on GNSS satellite observations. According to receiving signals from GNSS satellites, BG2s model is used as GNSS receiver for this research and made by the Institute of Geology and Geophysics, Chinese Academy of Sciences (IGGCAS). BG2s is designed to detect and analyze variations in the ionosphere, which can affect GNSS signal accuracy. It helps in calculating TEC and supports GNSS satellite systems, enabling broader coverage and more robust data collection over Thailand region.
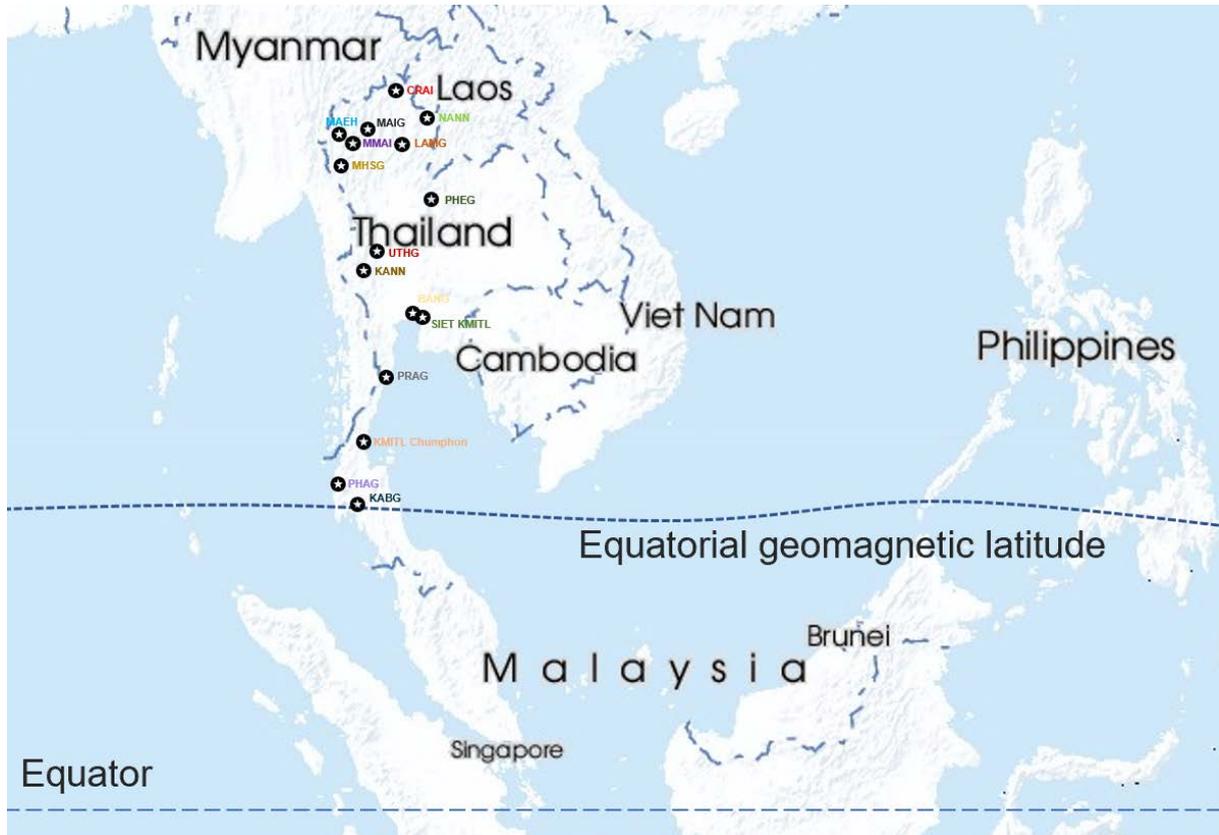

Figure 1. 16 GNSS receiver stations at low latitude, Thailand.

2.2 GNSS receiver bias model

To achieve accurate Total Electron Content (TEC) estimates, it is essential to properly eliminate frequency-dependent instrumental biases from both satellites and receivers in GNSS measurements. While satellite bias values are readily accessible online through various International GNSS Service (IGS) analysis centers, receiver biases – commonly referred to as differential code biases (DCBs) – are available only for a limited number of GNSS stations and select days. This limitation presents a significant challenge for TEC computation at individual stations. Numerous studies have explored DCB estimation methods, including works by Jin et al. (2012), Keshin (2012), Montenbruck et al. (2014), Zhang and Teunissen (2015), Jin et al. (2016), Wang et al. (2016), Choi and Lee (2018), Choi et al. (2019), Liu et al. (2019), Yuan et al. (2020), Wang et al. (2020), and Zhou et al. (2020). Building on this foundation, Arikan et al. (2008) developed and implemented IONOLAB-BIAS – an online algorithm designed to estimate receiver bias for single stations, providing both daily and monthly averages. IONOLAB-BIAS has been applied across a range of ionospheric conditions, from quiet to disturbed days, and for stations located in high-latitude, mid-latitude, and equatorial regions. Its receiver bias estimates have been benchmarked against two widely used offline methods and the limited receiver bias data available from IGS centers. Results show that IONOLAB-BIAS aligns closely with IGS estimates across all ionospheric conditions and geographic regions. With its

user-friendly implementation and reliable accuracy, IONOLAB-BIAS presents a strong alternative for single-station TEC estimation. There are various receiver bias estimation algorithms, and the most common used method can be roughly grouped into two methods as follows

In this approach, Vertical Total Electron Content (VTEC) is represented as a polynomial function based on the coordinates of the ionospheric pierce point, defined within a coordinate system aligned with the Earth-Sun axis (Lanyi and Roth, 1988). These pierce point coordinates are derived using angular relationships between the satellite and GPS receiver positions, along with the assumed height of the ionospheric thin shell, as described by Lanyi and Roth. Similarly, Slant Total Electron Content (STEC) is modeled as a polynomial function of the angular differences between these coordinates as follows

$$STEC_u^m(n) = o_u^m + M\big(\in_m (n)\big)\big(c_1 + c_2\bar{\phi}_p + c_3\bar{\theta}_p + c_4\bar{\phi}_p^2 + c_5\bar{\phi}_p\bar{\theta}_p + c_6\bar{\theta}_p^2\big) \tag{1}$$

where o_u^m denotes the sum of satellite and receiver biases where subscript u and superscript m denote receiver and satellite, respectively. The function $\in_m (n)$ can be computed from satellite-receiver geometry using satellite ephemeris data, $\bar{\phi}_p$, and $\bar{\theta}_p$ are longitude and latitude respectively, c_1, i = 1,...,6 are the coefficients that form the VTEC polynomial.

Once the slant TEC is computed, the vertical TEC, VTEC, can be obtained using the thin shell approximation of Single Layer Ionosphere Model (SLIM) as

$$VTEC_u^m(n) = \frac{STEC_u^m(n)}{M\big(\in_m (n)\big)} \tag{2}$$

The mapping function $M(\in_m)$ is

$$M\big(\in_m (n)\big) = \left[1 - \left(\frac{R\cos\lambda(n)}{R + h}\right)^2\right]^{-1/2} \tag{3}$$

where λ is the satellite elevation angle, R is the earth radius of 6,378.137 km and h is the ionospheric shell height of 428.8 km (Schaer, 1999).

The polynomial coefficients and offset values can be obtained using a least squares approximation separately for nighttime and daytime measurement sessions. The satellite ephemeris data and satellite biases are widely available in IONEX files from IGS centers. For each satellite and time index for the chosen two hours duration, Eq. (1) is formed. For example, for satellite m_1 and time index n_1, Eq. (1) takes the form of

$$STEC_u^{m_1}(n_1) = o_u^{m_1} + M\left(\in_{m_1} (n_1)\right)\left(VTEC_u^{m_1}(n_1)\right) \tag{4}$$

where

$$VTEC_u^{m_1}(n_1) = c_1 + c_2\bar{\phi}_p^{m_1}(n_1) + c_3\bar{\theta}_p^{m_1}(n_1) + c_4\left[\bar{\phi}_p^{m_1}(n_1)\right]^2 + c_5\bar{\phi}_p^{m_1}(n_1)\bar{\theta}_p^{m_1}(n_1) + c_6\left[\bar{\theta}_p^{m_1}(n_1)\right]^2$$

When Eq. (4) is written for M_t satellites and N_t measurement samples, $M_t \times N_t$ equations are obtained for one observation session. Then, the total bias, o_u^m, and coefficients $c_1, c_2, c_3, c_4, c_5, c_6$ are solved using least squares. Since the o_u^m value is different for each satellite, satellite biases obtained from IONEX files are removed from these median values to compute receiver bias. Then, the median of these receiver bias values over the 24 hours period are taken to obtain a single daily receiver bias value.

An alternative approach for estimating receiver bias involves minimizing the standard deviation of Vertical Total Electron Content (VTEC) values derived from multiple satellites, as proposed by Ma and Maruyama (2003). This technique can be applied to data from either a single receiver or a network of receivers. It operates under the assumption that VTEC values obtained from all visible satellites should be equal, given that the measurements occur simultaneously and follow similar vertical paths through the ionosphere. This assumption holds true when satellite and receiver biases are accurately removed from the GPS data. Additionally, most VTEC estimation methods rely on the premise of ionospheric spatial homogeneity across a broad range of elevation and azimuth angles, along with temporal stationarity over intervals of 5 to 15 minutes (Arikan et al., 2003). In practice, this method involves testing a range of receiver bias values and computing VTEC for each. The optimal bias is identified as the one that yields the minimum standard deviation of VTEC across satellites, indicating consistency in the measurements (Ma and Maruyama, 2003). The procedure for calculating the standard deviation of VTEC during a measurement period is detailed in Ma and Maruyama (2003) as Eq. (5)

$$\sigma_{t,u} = \sum_{n=1}^{N_t} \sigma_u(n)$$

(5)

where $\sigma_{t,u}$ is a total standard deviation of TEC and

$$\sigma_u(n) = \sqrt{\frac{1}{M_t} \sum_{n=1}^{M_t} \left(VTEC_u^m(n) - \overline{VTEC}_u(n) \right)^2}$$

M_t denotes the total number of satellites and N_t is duration of the desired measurement time interval in samples. The total standard deviation is obtained by summing the standard deviation value of each measurement samples where N_t is selected as 24 hours, corresponding to 2880 GPS measurements. $\overline{VTEC}_u(n)$ denotes the average of all VTEC from M_t satellites. To estimate the receiver bias, a range of trial values from −30 ns to +30 ns is tested in increments of 0.001 ns. For each receiver bias value, VTEC and the corresponding total standard deviation $\sigma_{t,u}$ are computed using the Eq. (5). The receiver bias that results in the minimum total standard deviation is selected as the optimal value.

In practical computation, GNSS TEC values were obtained from the Receiver Independent Exchange (RINEX) format. In this study, TEC was calculated using an observation file of GNSS parameters, including L_1, L_2, P_1 (C_1), and P_2. The VTEC is obtained by computing the STEC. VTEC is measured in TEC units (1 TECU = 10^{16} el/m^2) and is based on the total number of electrons in a one-square-meter tube along the signal channel. We used Eqs. (6) and (7) for GNSS TEC, VTEC, or TEC computation with MATLAB programming. Equation (6), $STEC_L$ can be used to determine the phase difference (L_1 and L_2) between the two frequencies (f_1 and f_2) to obtain STEC from satellites to the receiver (Ma and Maruyama, 2003; Kenpankho et al., 2011).

$$STEC_L = \frac{2(f_1 f_2)^2}{k(f_1^2 - f_2^2)} (L_1 \lambda_1 - L_2 \lambda_2)$$

(6)

where the wavelengths λ_1 (0.1904 m) and λ_2 (0.2444 m) for GPS, λ_1 (0.1921 m) and λ_2 (0.2485 m) for BeiDou, λ_1 (0.1900 m) and λ_2 (0.2550 m) for Galileo, λ_1 (0.1860 m) and λ_2 (0.2390 m) for GLONASS, and k, which are related to ionosphere refraction ($k = 80.62$ m^3/s^2), correspond to frequencies f_1 (1575.42 MHz) and f_2 (1227.60 MHz) for GPS, frequencies f_1 (1561.98 MHz) and f_2 (1207.14 MHz) for BeiDou, frequencies f_1 (1575.42 MHz) and f_2 (1176.45 MHz) for Galileo, and frequencies f_1 (1602.00 MHz) and f_2 (1246.00 MHz) for GLONASS. Furthermore, using Eq. (7), the VTEC is calculated in el/m^2 (Ma and Maruyama, 2003; Kenpankho et al., 2011).

$$\text{VTEC} = (\text{STEC} - b_s - b_r) \times \cos\chi, \tag{7}$$

where b_s and b_r are the estimated satellite and receiver biases and where χ is the satellite elevation angle. For this point of view, the VTEC is TEC. When TEC is obtained from GNSS signals, TEC can be called GNSS TEC. In the outline of VTEC computation, the GNSS receiver bias is needed to be solved. At this moment, it is not easy to find the receiver's biases. For finding receiver biases for one day, it probably takes in one hour due to try out the receiver bias values. So, we use about 30 hours to find a GNSS receiver bias for a month.

For GNSS satellites, there are two problems which need to be solved on finding GNSS receiver bias. One is to reduce the complexity of GNSS receiver bias estimation and the other is to find the GNSS receiver bias estimation at the missing points. For solving those problems, the GNSS receiver bias method is proposed. The method is for reducing the complexity of GNSS receiver bias estimation and estimating the receiver bias for a missing point. At the preparing data set, the median cut is applied from the minimization of standard deviation of Vertical TEC (VTEC). For this step, the GNSS receiver bias is assumed to be consistent value in every 15 minutes. The receiver bias is obtained from the median cut. The GNSS receiver biases are in ns units which are obtained from the RINEX file at 16 stations during the year 2022-2024 for GNSS satellite. The medians of GNSS receiver biases are 96 values a day during the year 2004-2024. For the daily median GNSS receiver biases, x is a time point and y is a median bias for GNSS satellites. The daily median GNSS receiver biases are plotted against 15 minutes time points. For the proposed method, the GNSS receiver bias estimation is calculated by using the 5th order Lagrange interpolation (Kenpankho et al., 2021) in Eq. (8).

$$y(x) = \sum_{i=0}^{5} \left(\prod_{\substack{j=0 \\ j \neq 1}}^{5} \frac{x - x_j}{x_i - x_j} y(x_i) \right) \tag{8}$$

According to the Lagrange interpolation method, six important points for daily median GNSS receiver biases, the first point, pre-sunrise point, noontime point, post-sunset point, midnight point, and the last point in each day, are selected from the daily median 15 minutes GNSS receiver biases as follows: $x_0 = 1$, $y(x_0) = -3$, $x_1 = 16$, $y(x_1) = -4$, $x_2 = 43$, $y(x_2) = -6$, $x_3 = 64$, $y(x_3) = -4.75$, $x_4 = 80$, $y(x_4) = -5.25$, and $x_5 = 96$, $y(x_5) = -4.75$. Then, the proposed model for GNSS receiver bias is defined as follows Eq. (9).

$$y(x) = -3.177179993438 + 0.167520974463x - 0.026621541654x^2 + 0.000081300189x^3 - \\ - 0.000000955941x^4 + 0.0000000038868x^5, \qquad 1 \leq x \leq 96 \tag{9}$$

This proposed method, the time is required to be selected to find the GNSS receiver bias. Selected time can be outside of 15 minutes interval. The model is required to chose the time for finding the GNSS receiver biases. For instance, if the selected time is 0:06 UTC, then time point for finding GNSS receiver bias is scaled and the result of GNSS receiver bias is calculated as following. Let UTC time at 0:15 be 1, then, 0:06 for x is 0.4.

$$y(0.4) = -3.177179993438 + 0.167520974463(0.4) - 0.026621541654(0.4)^2 + 0.000081300189(0.4)^3 - \\ - 0.000000955941(0.4)^4 + 0.0000000038868(0.4)^5 = -3.1145$$

Then, the estimated GNSS receiver bias at 0:03 UTC is -3.1145 ns which is used for finding TEC. The GNSS receiver bias model is developed to estimate receiver biases, producing over 2,880 bias values determined by the selected time interval. The advantages of proposed model are that the complexity of finding GNSS receiver bias is reduced and the time of GNSS receiver bias estimation at a specified time can be achieved as well.

2.3 RI-2020 model

The IRI Total Electron Content (IRI TEC) model, developed by the International Reference Ionosphere (IRI) which is a globally coordinated scientific initiative jointly sponsored by the Committee on Space Research (COSPAR) and the International Union of Radio Science (URSI). Developed through decades of international collaboration, the IRI model considered as the official standard for ionospheric parameters, offering a comprehensive empirical representation of Earth's ionosphere from altitudes of 50 km to 2,000 km. It integrates data from ground-based ionosondes, incoherent scatter radars, satellite mission, and rocket experiments to provide robust climatological profiles of ion and electron densities, temperatures, and ion composition. IRI TEC, accessible via NASA's Community Coordinated Modeling Center (CCMC) at https://kauai.ccmc.gsfc.nasa.gov/instantrun/iri/, currently hosts the IRI-2020 version. This version incorporates updated algorithms and datasets to enhance the accuracy of TEC predictions. In this study, we employed the IRI TEC 2020 model with NeQuick topside correction model and URSI-88 coefficients model to investigate observed GNSS TEC in GNSS receiver bias model for TEC monitoring at low latitude, Thailand, over a period of 2022-2024. By inputting location-specific and time-specific parameters, we extracted TEC profiles and analyzed their temporal behavior to assess ionospheric dynamics and their implications for GNSS receiver bias model performance.

3. Results and Comparisons

3.1 TEC results

GNSS TEC values measured by using proposed GNSS receiver bias model across 16 stations in Thailand from 2022 to 2024 show a consistent upward trend in ionospheric activity as shown in Table 2 and Fig. 2. In Bangkok, TEC ranged from a low of 5 TECU to a high of 32 TECU in 2022, increasing to 10-50 TECU in 2023 and 18-70 TECU in 2024. Chiangmai recorded 5-37 TECU in 2022, 9-60 TECU in 2023, and 15-85 TECU in 2024. Chiangrai rose from 5-32 TECU in 2022, 12-52 TECU in 2023, and 16-83 TECU in 2024. Kanchanaburi rose from 6-35 TECU in 2022, 11-52 TECU in 2023, and 20-70 TECU in 2024. KMITL Chumphon increased from 5-33 TECU in 2022 to 11-52 TECU in 2023 and 18-70 TECU in 2024. Krabi's TEC values moved from 5-30 TECU in 2022 to 10-43 TECU in 2023 and 17-61 TECU in 2024. Lampang rose from 5-35 TECU in 2022 to 10-60 TECU in 2023 and 15-78 TECU in 2024. MaeChaem in Chiangmai matched this trend with 5-38 TECU in 2022, 10-60 TECU in 2023, and 15-84 TECU in 2024. Maehongson recorded 5-38 TECU in 2022, 8-62 TECU in 2023, and 15-84 TECU in 2024. MaeSaring increased from 5-35 TECU in 2022 to 10-60 TECU in 2023 and 15-80 TECU in 2024. Nan's TEC values rose from 5-36 TECU in 2022 to 9-63 TECU in 2023 and 15-83 TECU in 2024. Phangnga showed 8-31 TECU in 2022, 10-45 TECU in 2023, and 17-63 TECU in 2024. Phetchabun recorded 6-38 TECU in 2022, 11-57 TECU in 2023, and 16-78 TECU in 2024. Prachuapkhirikan increased from 5-31 TECU in 2022 to 9-48 TECU in 2023 and 17-64 TECU in 2024. SIET KMITL rose from 5-33 TECU in 2022 to 11-51 TECU in 2023 and 18-69 TECU in 2024. Finally, Uthaithani's TEC values climbed from 5-33 TECU in 2022 to 11-55 TECU in 2023 and 17-72 TECU in 2024. These results reflect a clear intensification of ionospheric electron content over the period of year 2022-2024, with both high and low TEC values rising across all stations.

In Fig. 3, from 2022-2024, seasonal TEC variations across 16 stations in Thailand reveal consistent diurnal patterns and seasonal dependencies. TEC values typically rise from morning, peak around 12-15 LT, and decline toward evening. Equinox seasons consistently show the highest TEC levels, especially in 2024, with peak values reaching approximately 170 TECU at KMITL Chumphon. Summer seasons follow colsely, with 2023 often showing the highest TEC among the three years, peaking around 120 TECU at MaeChaem, Chiangmai. Winter seasons exhibit the lowest TEC values across all stations and years, with 2022 generally recording the maximum at 160 TECU at KMITL Chumphon. Among all stations, northern and central locations such as MaeChaem, Chiangmai, Chiangmai, Chiangrai, and Phetchabun tend to show stronger TEC peaks during Equinox, while southern stations like Krabi and Phangnga display slightly lower TEC. Overall, the results highlight that 2024 stands out as the year with the highest TEC across most stations during Equinox, and 2022 as the year with the lowest TEC during Winter, emphasizing the combined influence of solar activity, seasonal dynamics, and geographic location on ionospheric electron density over Thailand.

Table 2. A consistent upward trend in ionospheric activity during the year 2022-2024.

Stations	Upward trend (TECU)		
	2022	2023	2024
Bangkok	5-32	10-50	18-70
Chiangmai	5-37	9-60	15-85
Chiangrai	5-32	12-52	16-83
Kanchanaburi	6-35	11-52	20-70
KMITL Chumphon	5-33	11-52	18-70
Krabi	5-30	10-43	17-61
Lampang	5-35	10-60	15-78
MaeChaem, Chiangmai	5-38	10-60	15-84
Maehongson	5-38	8-62	15-84
MaeSariang	5-35	10-60	15-80
Nan	5-36	9-63	15-83
Phangnga	8-31	10-45	17-63
Phetchabun	6-38	11-57	16-78
Prachuapkhirikhan	5-31	9-48	17-64
SIET KMITL	5-33	11-51	18-69
Uthaithani	5-33	11-55	17-72

(a) Bangkok

(b) Chiangmai

(c) Chiangrai

(d) Kanchanaburi

(e) KMITL Chumphon

(f) Krabi

(g) Lampang

(h) MaeChaem, Chiangmai

(i) Maehongson

(j) MaeSariang

(k) Nan

(l) Phangnga

(m) Phetchabun

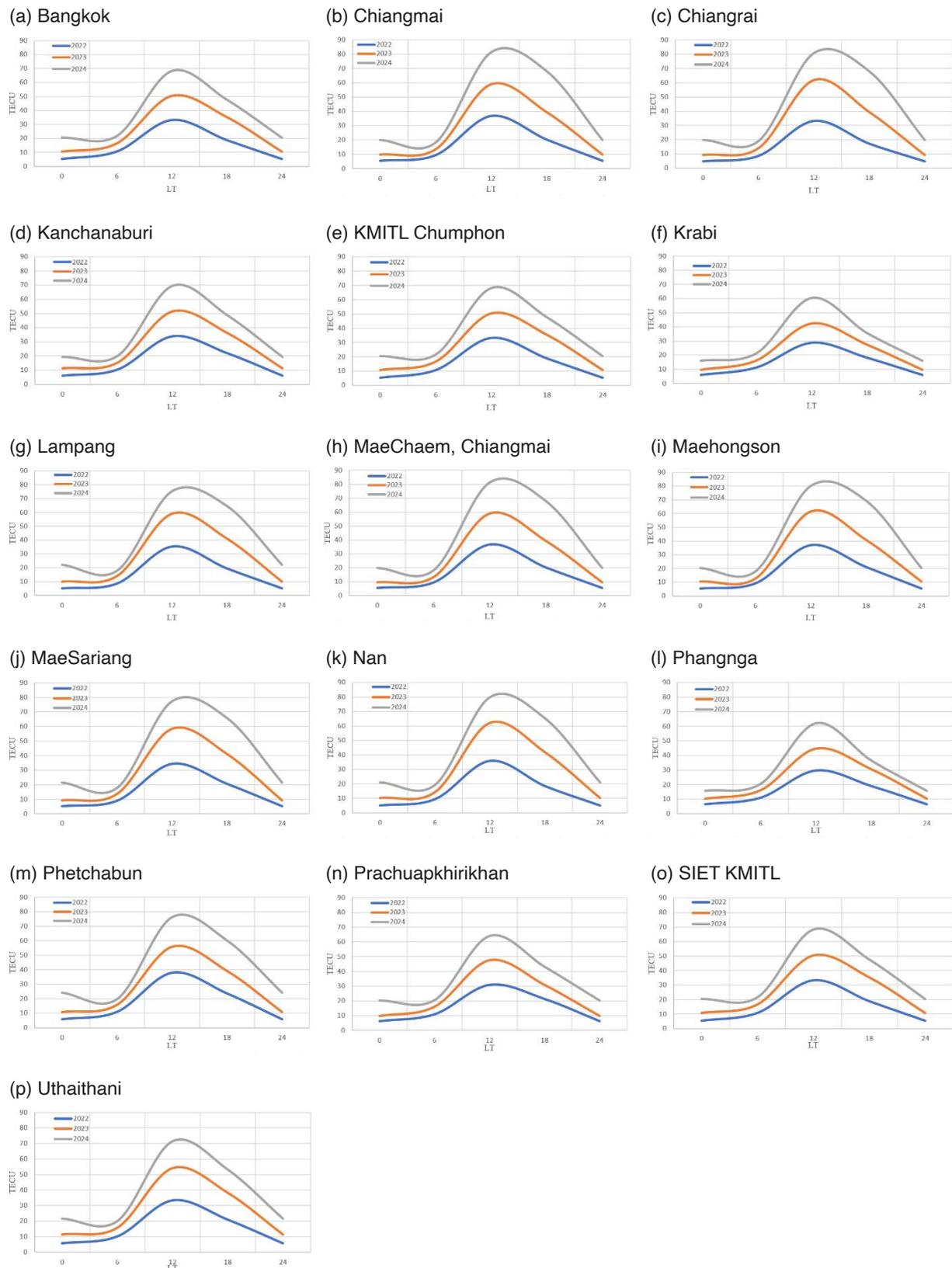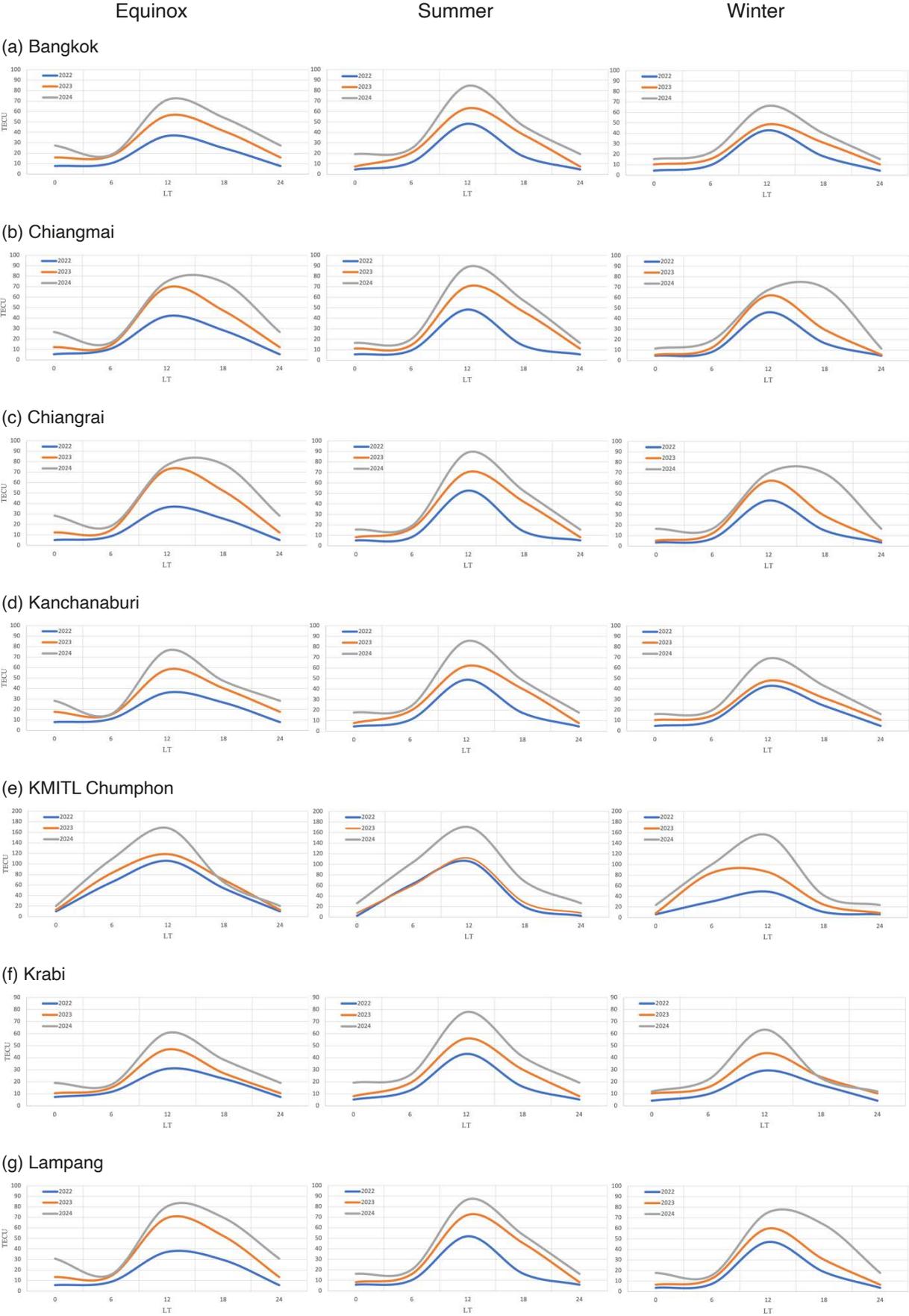(n) Prachuapkhirikhan

(o) SIET KMITL

(p) Uthaithani

Figure 2. TEC variations at 16 stations for the period of 2022-2024.

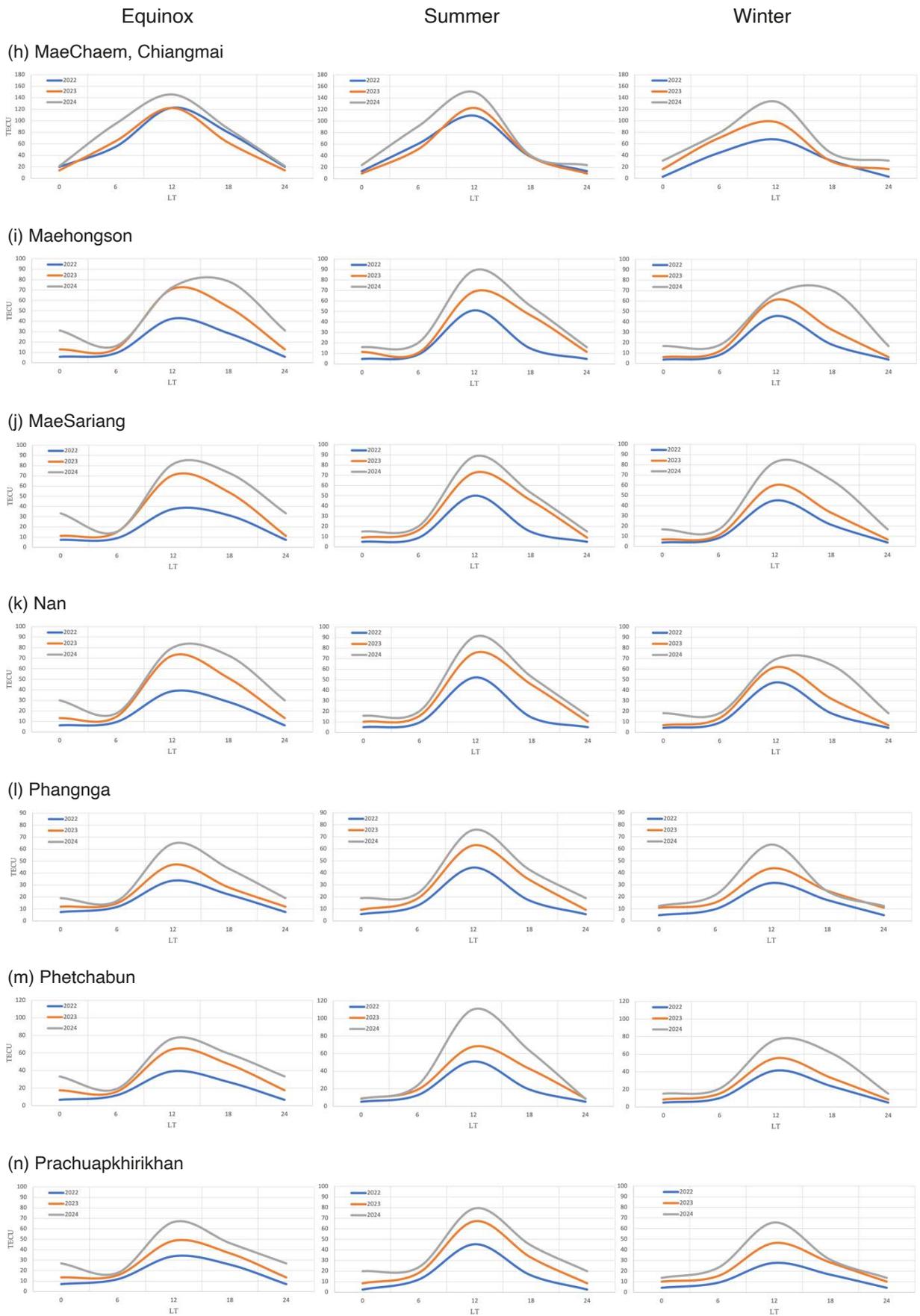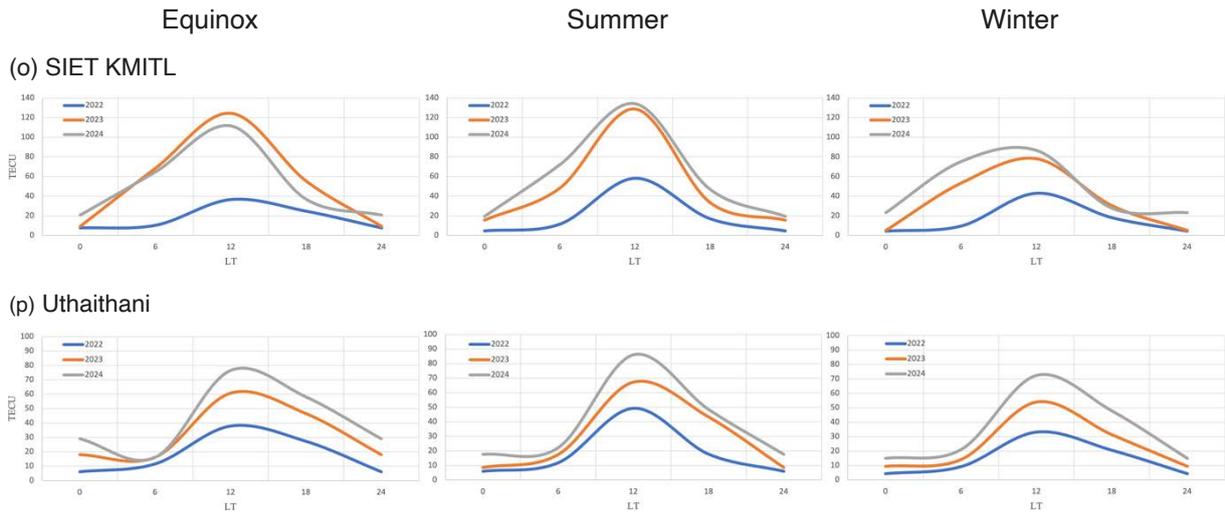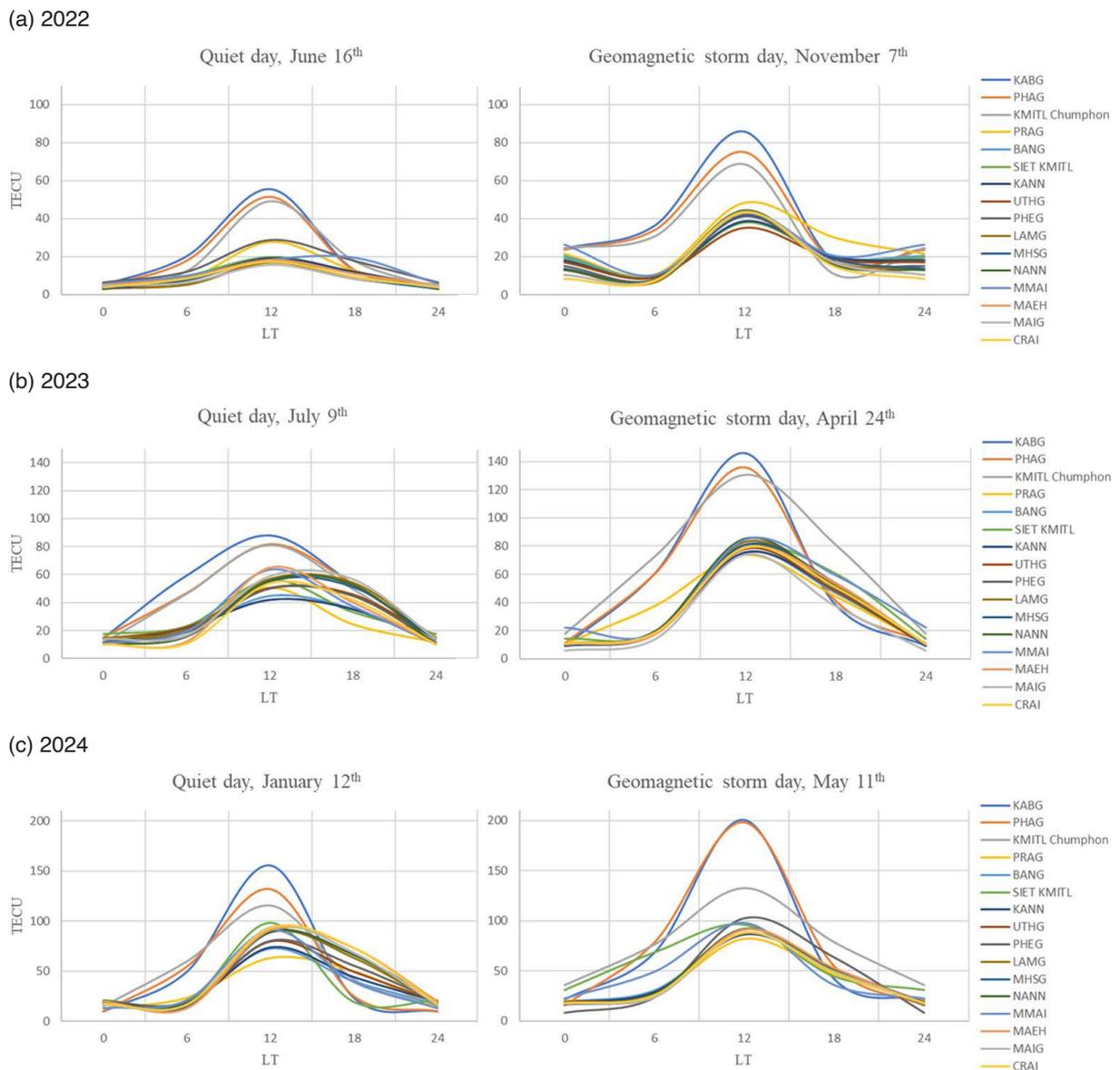**Figure 3.** Seasonal TEC variations at 16 stations for the period of 2022-2024.

	Equinox	Summer	Winter

(h) MaeChaem, Chiangmai

(i) Maehongson

(j) MaeSariang

(k) Nan

(l) Phangnga

(m) Phetchabun

(n) Prachuapkhirikhan

Figure 3. Seasonal TEC variations at 16 stations for the period of 2022-2024 (continued).

Equinox   Summer   Winter

(o) SIET KMITL

(p) Uthaithani

Figure 3. Seasonal TEC variations at 16 stations for the period of 2022-2024 (continued).

(a) 2022

(b) 2023

(c) 2024

Figure 4. TEC variations on quiet and geomagnetic days at 16 stations for the period of 2022-2024.

In Fig. 4, across all GNSS stations from 2022 to 2024, the TEC variations show distinct differences between the selected quiet days and geomagnetic storm days, with clear year to year increases linked to rising solar activity. In 2022, Fig. 4(a), the quiet day on 16 June, Dst −10 nT, shows nighttime minima of about 5-8 TECU, lowest at MAIG, and midday peak of about 55 TECU, highest at KABG, while the storm day on 7 November, Dst −90 nT, raises the peak to about 85 TECU, highest at KABG, with nighttime values near 10 TECU, lowest at CRAI. In 2023, Fig. 4(b), the quiet day on 9 July shows, Dst −6 nT, midday peaks of about 90 TECU, highest at KABG, and nighttime minima of about 12 TECU, lowest at CRAI, whereas the storm day on 24 April, Dst −213 nT, increases the peak to about 145 TECU, highest at KABG,with the lowest nighttime TEC (about 10 TECU) observed at MAIG. By 2024, Fig. 4(c), a year close to solar maximum, the quiet day on 12 January, Dst −4 nT, displays strong midday peaks of about 150 TECU, highest at KABG, with nighttime minima (about 12 TECU) again lowest at MAEH, while the storm day on 11 May, Dst −406 nT, produces the largest TEC enhancement in the datasets, reaching 200 TECU, highest at KABG, and maintaining nighttime minima of 15 TECU, lowest at MAIG. Overall, the results show that storm days consistently elevate TEC above quiet day levels, the highest TEC in each year is always recorded at low latitude or equatorial proximal stations (KABG, PHAG, KMITL Chumphon), the lowest TEC values typically occur at more upper low latitude stations (CRAI, MAIG, MAEH), and the strongest ionospheric response occurs during the geomagnetic storm of 11 May 2024.

3.2 TEC comparison

For TEC comparison between GNSS TEC derived from RINEX files by using the proposed GNSS receiver bias model and IRI 2020 TEC from IRI-2020 model, the comparisons were used TEC correlation coefficient and Root Mean Square Error (RMSE). In Table 3 and Fig. 5, the correlation coefficient between GNSS TEC and IRI TEC across 16 stations in Thailand from 2022 to 2024 reveal notable spatial and temporal variations. In 2022, the highest correlations were observed at SIET KMITL and Chiangrai (both at 0.89), followed closely by Bangkok (0.88) and MaeSaring (0.86), indicating strong agreement between GNSS and IRI TEC models in their regions. Conversely, Phetchabun recorded the lowest correlation at 0.58, suggesting greater discrepancies. By 2023, most stations maintained moderate to high

Table 3. TEC correlation coefficient between GNSS TEC and IRI TEC.

Stations	TEC correlation coeficient		
	2022	2023	2024
Bangkok	0.88	0.79	0.74
Chiangmai	0.69	0.78	0.61
Chiangrai	0.89	0.78	0.54
Kanchanaburi	0.75	0.77	0.72
KMITL Chumphon	0.73	0.79	0.80
Krabi	0.70	0.80	0.74
Lampang	0.80	0.78	0.61
MaeChaem, Chiangmai	0.71	0.79	0.68
Maehongson	0.73	082	0.52

Stations	TEC correlation coeficient		
	2022	2023	2024
MaeSariang	0.86	0.76	0.54
Nan	0.83	0.72	0.70
Phangnga	0.68	0.78	0.79
Phetchabun	0.58	0.77	0.85
Prachuapkhirikhan	0.82	0.83	0.70
SIET KMITL	0.89	0.80	0.76
Uthaithani	0.68	0.77	0.61

correlations, with Prachuapkhirikhan peaking at 0.83 and Maehongson showing a strong 0.82. However, some stations like Nan and Chiangrai experienced slight declines, while others such as Krabi and KMITL Chumphon improved. In 2024, the trend shifted further, with Phetchabun showing a remarkable increase to 0.85, the highest among all stations in this year, indicating improved model alignment. KMITL Chumphon and Phangnga also maintained high correlations at 0.80 and 0.79, respectively. Meanwhile, several northern stations such as Chiangrai, Maehongson, and MaeSariang saw significant drops, falling to 0.54 or lower, which may reflect increased ionospheric variability or model limitations in those areas. Overall, while some stations demonstrated consistent performance across the years, other exhibited fluctuations that highlight the dynamic nature of TEC behavior and the varying accuracy of IRI models across different geographic locations.
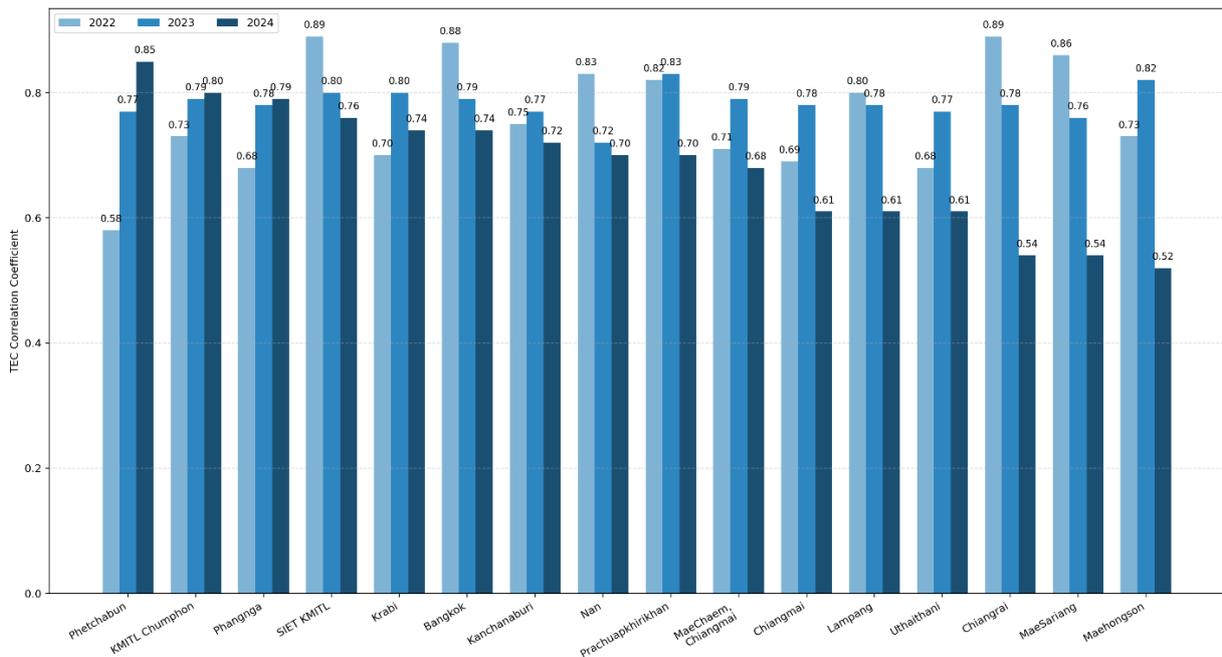

Figure 5. TEC correlation coefficient comparative plot between GNSS TEC and IRI TEC.

In Table 4 and Fig. 6, the RMSE values between GNSS TEC and IRI TEC across 16 stations from 2022 to 2024 reveal a consistent upward trend, indicating increasing discrepancies between observed TEC values using GNSS receiver bias model and modeled TEC values over time. In 2022, most stations exhibited moderate RMSEs, with Nan showing the highest error at 7.07 TECU, while Uthaithani had the lowest at just 0.99 TECU, suggesting excellent model performance there. Coastal stations like Krabi and Phangnga also recorded relatively low RMSEs (1.83 and 3.97 TECU, respectively), while urban centers such as Bangkok and Chiangmai had higher errors around 4.61 and 5.04 TECU. In 2023, RMSE rose notably across nearly stations. Maehongson experienced a sharp increase to 9.44 TECU, the highest this year, followed closely by Chiangrai and Chiangmai, both exceeding 7.5 TECU. KMITL Chumphon and SIET KMITL remained below 6.5 TECU, showing relatively stable performance. In 2024, the trend continued, with Chiangmai reaching the peak RMSE of 10.66 TECU, followed by Chiangrai (10.41 TECU) and Maehongson (9.92 TECU), indicating significant divergence from IRI predictions in northern regions. Meanwhile, Uthaithani maintained the lowest RMSE across all years, rising only slightly to 1.66 TECU in 2024. These results suggest that while some stations consistently align well with IRI TEC models, others particularly in upper low latitude areas, show increasing deviation, possibly due to complex ionospheric dynamics affecting TEC variability.

Table 4. RMSE between GNSS TEC and IRI TEC.

| Stations	RMSE (TECU)		
	2022	2023	2024
Bangkok	4.61	6.25	7.20
Chiangmai	5.04	7.55	10.66
Chiangrai	5.01	7.59	10.41
Kanchanaburi	4.91	6.85	9.37
KMITL Chumphon	3.98	5.95	7.89
Krabi	1.83	2.49	3.47
Lampang	2.83	3.87	5.44
MaeChaem, Chiangmai	4.98	7.35	9.90
Maehongson	4.96	9.44	9.92
MaeSariang	2.88	3.95	5.34
Nan	7.07	8.30	8.92
Phangnga	3.97	5.83	7.78
Phetchabun	2.62	3.63	5.06
Prachuapkhirikhan	4.33	6.39	8.48
SIET KMITL	4.50	6.20	7.10
Uthaithani	0.99	1.15	1.66
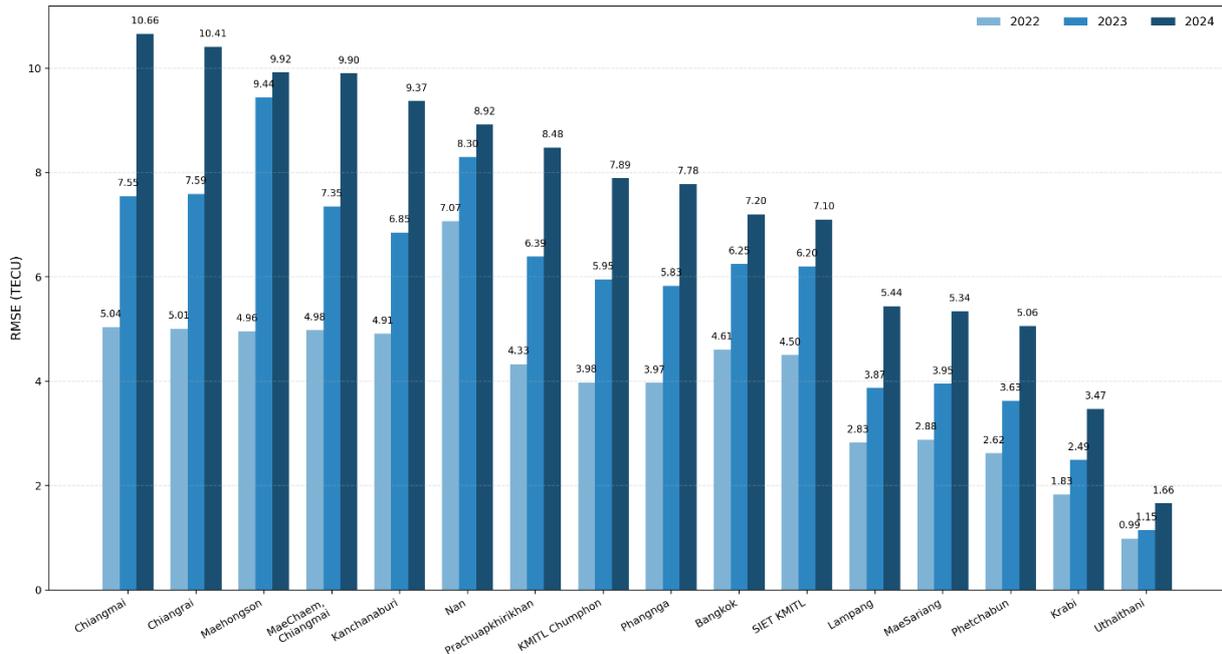
Figure 6. RMSE comparative plot between GNSS TEC and IRI TEC.

4. Discussion

The GNSS TEC results across 16 stations, low latitude, in Thailand from 2022 to 2024 demonstrate a clear upward trend in ionospheric activity, season, quiet and geomagnetic days, consistent with increased solar activity during this period. This trend is evident in both low and high TECU values, with stations such as Chiangmai, Chiangrai, and Maehongson showing particularly strong increase. These findings along with previous studies emphasize the dynamic nature of ionospheric behavior in low latitude regions (Ma and Maruyama, 2003; Kenpankho et al., 2011). The use of the proposed GNSS receiver bias model significantly enhances TEC estimation accuracy by addressing inter-frequency biases, particularly differential code biases (DCBs), which are often underrepresented in standard models (Otsuka et al., 2002; Warnant, 1997). The integration of IONOLAB-BIAS for single stations bias estimation further strengthens the methodology, offering reliable daily and monthly bias values that correlate well with IGS benchmarks (Arikan et al., 2008). Comparative analysis with the IRI 2020 model reveals spatial and temporal variations in TEC correlation coefficients. Stations such as SIET KMITL and Chiangrai exhibited high correlations in 2022 (0.89), indicating strong agreement with IRI model. However, by 2024, several northern stations, including Chiangrai and Maehongson, upper low latitude, showed notable declines in correlation (0.54 and 0.52, respectively), suggesting increased ionospheric variability or limitations in the IRI model's regional performance. RMSE values further highlight these discrepancies. While coastal, near equatorial latitude, like Krabi and central station, low latitude, like Uthaithani maintained low RMSEs across all years, northern stations such as Chiangmai and Chiangrai, upper low latitude, experienced significant increases, peaking at 85 TECU and 83 TECU in 2024, respectively. These results underscore the importance of localized TEC modeling, especially in regions with complex ionospheric dynamics (Zhang et al., 2015; Wang et al., 2021). Overall, the study confirms that multi-frequency GNSS observations, when corrected for receiver biases, provide a robust framework for near real-time TEC monitoring. The observed TEC trends and model comparisons emphasize the need for adaptive ionospheric models that account for regional and temporal variability.

5. Conclusion

This research study successfully applied a GNSS receiver bias model to monitor and analyze TEC variations across 16 stations, low latitude, in Thailand from 2022 to 2024. The results reveal a consistent increase in TEC values,

reflecting heightened latitudes, solar and ionospheric activity, seasons, and geomagnetic storms. By correcting for satellite and receiver biases, particularly through the use of IONOLAB-BIAS, the model achieved improved TEC estimation accuracy. Comparisons with the IRI 2020 model showed strong correlations at several stations, though discrepancies emerged in upper low latitude regions, highlighting the limitations of global models in capturing localized ionospheric behavior. The finding underscores the values of regional GNSS-based TEC monitoring systems for enhancing satellite navigation and positioning accuracy in low latitude environments.

Data availability statement. Data will be made available on request.

References

Arikan, F., C. B. Erol and O. Arikan (2003). Regularized estimation of vertical total electron content from Global Positioning System data, J. Geophys. Res.: Space Physics, 108, A12, 1469, doi:10.1029/2002JA009605.

Arikan, F., U. Sezen, O. Arikan, M. Ugur et al. (2008). IONOLAB-BIAS: A new technique and software for estimation of GPS receiver bias, Radio Sci., 43, RS6014, 1-12, doi:10.1029/2007RS003785.

Cao, J., X., Li and Y. Zhang (2021). Analysis of delay times between BeiDou-2 and BeiDou-3 satellites, Remote Sensing, 13, 1, 1-10., doi:10.3390/rs13010010.

Choi, B. K. and S. J. Lee (2018). Combined GPS/GLONASS relative receiver DCB estimation using the LSQ method and ionospheric TEC changes over South Korea. Journal of Positioning, Navigation, and Timing, 7, 3, 175-181, doi:10.11003/JPNT.2018.7.3.175.

Choi, B. K., D. H. Sohn and S. J. Lee (2019). Correlation between ionospheric TEC and the DCB stability of GNSS receivers from 2014 to 2016, Remote Sensing, 11, 22, 2657, doi:10.3390/rs11222657.

Coco, D. S., Coker, C., A. J. Mazzella and G. J. Bishop (1991). Algorithms that use the ionosphere to control GPS errors, IEEE Position Location and Navigation Symposium, 145-152.

Dandan, H., A. Krypiak-Gregorczyk, M. Hernández-Pajares, J., Kaplon et al. (2017). Impact and implementation of higher-order ionospheric effects on precise GNSS applications. Journal of Geophysical Research: Solid Earth, 122, 10, 9420-9436, doi:10.1002/2017JB014750.

Jakowski, N., E. Sardon and S. Schlüter (1996). GPS-based TEC observations in Europe, Ann. Geophys., 14, 9, 1025-1032, doi:10.1007/s00585-996-1025-3.

Jin, R., Jin, S. and G. Feng (2012). M_DCB: Matlab code for estimating GNSS satellite and receiver differential code biases, GPS Solutions, 16, 4, 541-548, doi:10.1007/s10291-012-0279-3.

Jin, S., R. Jin, and D. Li (2016). Assessment of BeiDou differential code bias variations from multi-GNSS network observations, Ann. Geophysicae, 34, 259-269, doi:10.5194/angeo-34-259-2016.

Kenpankho, P., A. Chaichana, K. Trachu, P. Supnithi and K. Hozumi (2021). Real-time GPS receiver bias estimation, Adv. Space Res., 68, 5, 2152-2159, doi:10.1016/j.asr.2021.01.032.

Kenpankho, P., K. Watthanasangmechai, P., Supnithi, T. Tsugawa and T. Maruyama, (2011). Comparison of GPS TEC measurements with IRI TEC prediction at the equatorial latitude station, Chumphon, Thailand. Earth, Pl. Space, 63, 365-370, doi:10.5047/eps.2011.01.010.

Keokhumcheng, T. and P. Kenpankho (2025). The study of total electron content on ionosphere by using single frequency GPS receiver, Adv. Space Res., 75, 5, 4245-4259, doi:10.1016/j.asr.2024.08.019.

Keshin, M. (2012). A new algorithm for single receiver DCB estimation using IGS TEC maps, GPS Solu., 16, 3, 295-303, doi:10.1007/s10291-011-0230-z.

Lanyi, G. E. and T. Roth (1988). A comparison of mapped and measured total ionospheric electron content using Global Positioning System signals, Radio Sci., 23, 3, 483-492, doi:10.1029/RS023i003p00483.

Li, X., M. Ge, X. Dai, X., Ren et al. (2015). Accuracy and reliability of multi-GNSS real-time precise positioning: GPS, GLONASS, BeiDou, and Galileo, J. Geod., 89, 6, 1-14, doi:10.1007/s00190-015-0802-8.

Liu, T., B. Zhang, Y. Yuan, Z. Li and N. Wang (2019). Multi-GNSS triple-frequency differential code bias (DCB) determination with precise point positioning (PPP), J. Geod., 93, 765-784, doi:10.1007/s00190-018-1194-3.

Ma, G. and T. Maruyama (2003). Derivation of TEC and estimation of instrumental biases from GEONET in Japan, Ann. Geophysicae, 21, 10, 2083-2093, doi:10.5194/angeo-21-2083-2003.

Makela, J. J., M. C. Kelley and J. W. Meriwether (2001). Simultaneous observations of the ionosphere and thermosphere from the Arecibo Observatory, J. Geophys. Res.: Space Phys., 106, A12, 29573-29583, doi:10.1029/2001JA000003.

Mallika, L. I., D. V. Ratnam, S. Raman and G. Sivavaraprasad (2020). Machine learning algorithm to forecast ionospheric time delays using GNSS observations, Acta Astronautica, 173, 221-231, doi:10.1016/j.actaastro.2020.04.048.

Montenbruck, O., A. Hauschild and P. Steigenberger (2014). Differential code bias estimation using multi-GNSS observations and global ionosphere maps, Navigation, 61, 3, 191-201, doi:10.1002/navi.64.

Otsuka, Y., T. Ogawa, A. Saito, T. Tsugawa et al. (2002). A new technique for mapping of total electron content using GPS network in Japan, Earth, Planets, Space, 54, 63-70, doi:10.1186/BF03352422.

Sardon, E., A. Rius and A. Zarraoa (1994). Estimation of the transmitter and receiver differential biases and the ionospheric total electron content from Global Positioning System observations, Radio Sci,, 29, 3, 577-586, doi:10.1029/94RS00449.

Schaer, S. (1999). Mapping and predicting the ionosphere using the Global Positioning System. Proceedings of the IGS Workshop 1998, Darmstadt, Germany. International GPS Service.

Srivani, I., G. S. V. Prasad and D. V. Ratnam (2019). A deep learning-based approach to forecast ionospheric delays for GPS signals, IEEE Geosci. Remote Sensing Lett., 16, 8, 1180-1184, doi:10.1109/LGRS.2019.2895112.

Wang, N., Z. Li, Y. Yuan and X. Huo (2021). BeiDou Global Ionospheric delay correction Model (BDGIM): Performance analysis during different levels of solar conditions, GPS Sol., 25, 97, doi:10.1007/s10291-021-01125-y.

Wang, N., Y. Yuan, Z. Li, O. Montenbruck and B. Tan (2016). Determination of differential code biases with multi-GNSS observations, J. Geod., 90, 209-228, doi:10.1007/s00190-015-0867-4.

Wang, Q., S. Jin and Y. Hu (2020). Epoch-by-epoch estimation and analysis of BeiDou Navigation Satellite System (BDS) receiver differential code biases with the additional BDS-3 observations, Ann. Geophysicae, 38, 1115-1122, doi:10.5194/angeo-38-1115-2020.

Warnant, R. (1997). Reliability of the TEC computed using GPS measurements: The problem of hardware biases, Acta Geodaetica et Geophysica Hungarica, 32, 3-4, 451-459.

Xiao, Y., Y. Zhang and J. Liu (2022). Development and assessment of atmospheric delay models for GPS, Galileo, and BDS PPP-RTK applications, Remote Sensing, 14, 1, 1-10, doi:10.3390/rs14010010.

Yuan, L., S. Jin and M. Hoque (2020). Estimation of LEO-GPS receiver differential code bias based on inequality constrained least square and multi-layer mapping function. GPS Sol., 24, 57, doi:10.1007/s10291-020-0970-8.

Zhang, B. and P. J. G. Teunissen (2015). Zero-baseline analysis of GPS/BeiDou/Galileo between-receiver differential code biases (BR-DCBs): Time-wise retrieval and preliminary characterization, Proceedings of the ION Pacific PNT Meeting, 107-116.

Zhang, R., W. Song, Y. Yao, C. Shi et al. (2015). Modeling regional ionospheric delay with ground-based BeiDou and GPS observations in China, GPS Sol., 19, 4, 649-658, doi:10.1007/s10291-014-0419-z.

Zhang, Y., F. Wu, N. Kubo and A. Yasuda (2003). "TEC measurement by single dual-frequency GPS receiver." International Symposium on GPS/GNSS, Tokyo, Japan, 15-18 Nov.

Zhou, Y., B. Zhang and P. J. G. Teunissen (2020). Characterization of multi-GNSS between-receiver differential code biases using zero and short baselines, Sci. Bull., 65, 22, 1840-1849, doi:10.1007/s11434-015-0911-z.

*CORRESPONDING AUTHOR: Prasert KENPANKHO,

Department of Engineering Education, School of Industrial Education and Technology,

King Mongkut's Institute of Technology Ladkrabang, Bangkok, Thailand.

e-mail: prasert.ke@kmitl.ac.th